Nanostructures

DOI: 10.1002/ange.200502823

Template-Free Synthesis and Assembly of Single-Crystalline Tungsten Oxide Nanowires and their Gas-Sensing Properties**

*Julien Polleux, Alexander Gurlo, Nicolae Barsan, Udo Weimar, Markus Antonietti, and Markus Niederberger**

The controlled synthesis and characterization of crystalline objects with reduced dimensionality is a fascinating objective in modern materials science, physics, and chemistry. One-dimensional systems such as nanowires and nanotubes are especially attractive building blocks for nanodevices because they represent the smallest dimension for efficient transport of electrons and excitons.[1] A wide variety of synthetic methodologies, ranging from vapor-phase techniques to solution-growth processes, have been used to produce nanowires of elements, oxides, nitrides, carbides, and chalcogenides.[2,3] Although transition metal oxides are an important class of materials,[4] soft-chemistry routes to crystalline metal-oxide nanowires under mild reaction conditions are not yet available. The reason for this is that sol-gel derived materials formed at low temperature are amorphous, and that the heat treatment necessary to induce crystallization is usually accompanied by an undesired alteration of the particle morphology.

In addition to the spontaneous self-assembly of preformed nanocrystals into nanowires by oriented attachment,[5–8] template techniques relying on the use of surfactants[9] or solids[10] as structure-directing agents have been reported for the soft-chemistry fabrication of anisotropic oxide nanomaterials. However, simpler systems avoid the use of additional templates, thereby enabling control over the dimensionality of the nanoparticles solely by the solvent, and thus offering the advantage that the amount of impurities in the final product can be kept low. The reaction of benzyl alcohol with metal alkoxides, for example, allows the controlled synthesis of metal oxide nanoparticles with a large variety of compo-

[*] Dr. J. Polleux, Prof. M. Antonietti, Dr. M. Niederberger
Max-Planck-Institute of Colloids and Interfaces
Research Campus Golm
14424 Potsdam (Germany)
Fax: (+49) 331-567-9502
E-mail: markus.niederberger@mpikg.mpg.de
Dr. A. Gurlo, Dr. N. Barsan, Dr. U. Weimar
University of Tuebingen
Institute of Physical and Theoretical Chemistry
Auf der Morgenstelle 15, 72076 Tuebingen (Germany)

[**] We thank Marc Willinger and Dr. Dangsheng Su (Fritz-Haber-Institute Berlin) for the HRTEM and Rona Pitschke for SEM measurements. Financial support by the Max-Planck-Society and by the DFG (priority program SPP 1165) is gratefully acknowledged.

Supporting information for this article is available on the WWW under http://www.angewandte.org or from the author.

sitions and particle shapes.[11–19] Similarly, benzylamine and *n*-butylamine can also act as shape-controlling agents.[20,21]

Herein, we report a soft-chemistry route to crystalline tungsten oxide nanowires self-assembled into bundles that is performed in a simple glass beaker at low temperature. Among the transition metal oxides, tungsten oxide offers a particularly wide spectrum of useful properties, including high structural flexibility,[22] switchable optical properties,[23] and catalytic behavior.[24] Accordingly, tungsten oxide is a good candidate for applications in electrochromic[25] and gas-sensing devices.[26,27] Anisotropic tungsten oxide nanorods have been prepared before using soft-chemistry approaches[28] and surfactant mixtures,[29–31] and additives such as oxalic acid or deferoxamine enabled the synthesis of self-assembled, highly oriented one-dimensional tungsten oxide nanostructures.[32,33] However, the absence of any structure-directing agents and the use of a halide-free precursor in our synthetic protocol, in combination with the outstanding aspect ratio of the nanowires, allows the preparation of a particularly promising nanomaterial for gas-sensing applications.

Tungsten isopropoxide in benzyl alcohol provides a versatile reaction system for the nonaqueous preparation of crystalline tungsten oxide nanowires. This one-pot synthetic procedure resulted in the formation of a blue powder, which was subsequently analyzed by XRD in the 2θ range of 2–60°. The corresponding powder pattern exhibits three sharp reflections (Figure 1a): the first reflection, centered at 4.68°

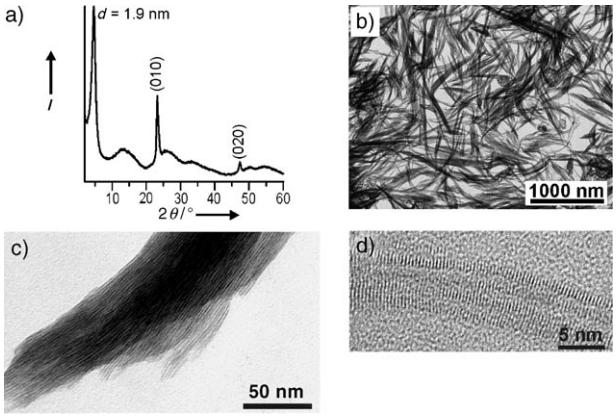

Figure 1. a) XRD powder pattern and b) TEM overview image of the as-synthesized tungsten oxide nanobundles. c) TEM image of a tip of one bundle consisting of individual nanowires. d) HRTEM image of a nanowire bundle.

in the small-angle range, corresponds to a *d*-value of 1.9 nm. The sharpness and intensity of the peak point to a highly ordered mesostructure. The other two reflections at $2\theta =$ 23.2° and 47.3° match best with the (010) and (020) planes of the monoclinic $W_{18}O_{49}$ (or $WO_{2.72}$) structure (JCPDS 36-101). All other reflections are much weaker, thus indicating that the nanowires grow along the [010] direction. Although it is difficult to assign the powder pattern unambiguously to a specific crystal structure as various stoichiometric and non-stoichiometric tungsten oxide compounds have rather similar structures,[22] the pattern is similar to that reported recently for $W_{18}O_{49}$ nanorods.[31]

A representative overview of the nanowire bundles is displayed in Figure 1b. Their length ranges typically from 300 to 1000 nm, although longer species were also found in the sample, and the width is between 20 and 100 nm. It is interesting to note that the entire sample consists of this anisotropic nanomaterial, with no indication of other products. The higher-magnification TEM image in Figure 1c gives evidence that the fibers consist of individual nanowires which appear with a dark contrast. Interestingly, the nanowires are mostly oriented parallel to each other with an equal distance almost throughout the whole length of the nanowires, giving rise to the intense reflection at $2\theta = 4.68°$. Accordingly, the constant interwire distance has to be a direct consequence of an ordered arrangement of the organic molecules between the inorganic nanowires. The high-resolution TEM image in Figure 1d shows lattice fringes characteristic of a crystalline material. The diameter of all nanowires is highly uniform, typically (1 ± 0.1) nm. This tiny size is comparable to the diameter of single-walled carbon nanotubes (typically around 1.2 nm).[34]

In order to learn more about the attractive forces between the individual nanowires, the tungsten oxide sample dispersed in ethanol was mixed with formamide. TEM investigations showed that the bundles are completely transformed into separate nanowires (Figure 2a), and only nanowires can be observed over a large area of the TEM grid (several square micrometers). A TEM image at higher magnification shows individual nanowires that are bent, sometimes forming circular structures (Figure 2b). The high flexibility of the nanowires can be explained by their small cross-section, as well as by the construction principle of tungsten oxide. Obviously, bending stress can be reduced by tilting the octahedra with respect to each other. Nevertheless, the

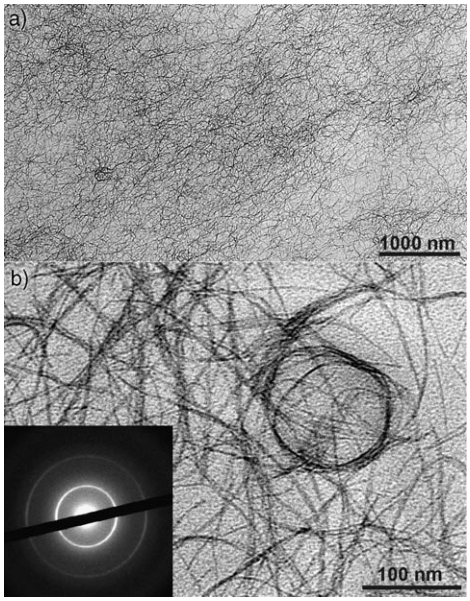

Figure 2. a) Overview TEM image of isolated nanowires. b) TEM image at higher magnification (inset: SAED pattern).

nanowires are crystalline, as proven by selected-area electron diffraction, which exhibits the two rings assigned to the (010) and (020) reflections (Figure 2b, inset).

The organization of the nanowires into bundles is directed by specific interactions between the organic species present in the reaction system, and the uniform distance between the nanowires indicates an ordered supramolecular arrangement of intercalated organic molecules. FTIR spectroscopy clearly proves the presence of an organic–inorganic hybrid structure in the nanowire bundles (see Supporting Information). The typical bands for W=O and bridging oxygens (O–W–O) appear in the region of 1000–500 cm^{-1} in the IR spectrum.[24] The bands at 1595, 1580, 1500, and 1451 cm^{-1} are characteristic of the skeletal vibrations of an aromatic ring,[24,35] whereas the band at 1207 cm^{-1} is typical of the C–C vibration.[35] However, the lack of a band at 1018 cm^{-1}, which represents the C–O stretch of benzyl alcohol,[35] and the presence of a strong band at 1690 cm^{-1}, assignable to C=O stretching, points to the possibility that benzyl alcohol has been partly oxidized to benzaldehyde or benzoic acid during nanowire growth. As a matter of fact, the position of the C=O band corresponds exactly to benzaldehyde adsorbed to the surface of metal oxides.[36] This value is shifted slightly to lower frequency in comparison to free benzaldehyde due to coordination to Lewis acid sites present at the surface of the tungsten oxide.[24] This observation is further supported by the fact that the bands for a carboxylate group, expected to be at around 1550 and 1410 cm^{-1},[24] are missing. Oxidation of benzyl alcohol to benzaldehyde with WO_3 powder as a catalyst is well known and occurs at low temperatures.[24] A similar oxidation step has also been observed in the reaction of benzyl alcohol with WCl_6 in the presence of deferoxamine mesylate,[33] although it is interesting to note that in the case of yttrium oxide synthesized in benzyl alcohol, the final inorganic–organic hybrid material consists of yttrium oxide layers with intercalated benzoic acid molecules.[19] In that example, the oxidation of benzyl alcohol did not stop at the aldehyde stage but proceeded to the acid. Thermogravimetric analysis of the fiber bundles shows a weight loss of about 16% in the range of room temperature to 540°C (see Supporting Information).

Chemical sensors play a profound role in the areas of public safety, emission control, and environmental protection. The ubiquitous presence of contaminants in the environment as well as the rigorous regulations on the emission of toxic gases demand local monitoring of low concentrations of polluting gases at many locations. The practical application of local monitoring requires the development of small and cheap sensing devices, with high sensitivities in the sub parts-per-million range. Semiconducting metal oxides as sensing elements feature several advantages, such as simplicity in device structure, low fabrication cost, robustness in practical applications, and adaptability to a wide variety of reducing and oxidizing gases.[26] The reduction of power consumption is gaining more and more importance in sensing applications, and demands for further miniaturization of sensor devices, and, consequently, the question of how sensors can be integrated with modern electronic fabrication technologies, becomes a serious issue. One-dimensional nanostructures such as nanowires and nanotubes are particularly promising in this regard because they provide a large surface-to-volume ratio, which should result in excellent sensitivities and fast recovery and response times. They are also easily configurable as field-effect transistors and integrable with conventional devices and device-fabrication techniques.[37] However, investigations on the gas-sensing properties of metal oxide nanowires are basically restricted to SnO_2[38–41] and In_2O_3,[40] mainly due to the lack of simple synthetic procedures for other crystalline and high-purity metal oxide nanowires.

The gas-sensing properties of the tungsten oxide nanowire bundles were studied, especially with regard to the assessment of the performance of the nanobundle-based sensors as potential candidates for detection of low levels of NO_2. The peculiar morphology of the tungsten oxide nanomaterial, combined with its small size, requires the optimization of many parameters for effective sensor generation. The thermal stability of the nanobundles, the compatibility of the deposition techniques with the "fragile" nanowire morphology, their conductivity, which is directly related to the stoichiometry and the crystallinity of the nanowires, as well as the right choice of the transducer/substrate structure have to be taken into account and still leave room for optimization. For the gas-sensing tests (see Supporting Information), a suspension of the tungsten oxide nanobundles in ethanol was deposited onto alumina substrates by drop-coating and subsequently calcined at 500°C in air, resulting in the formation of a highly porous network as sensing layers. According to SEM results, the morphology of the nanowire bundles prior to (Figure 3a) and after heat treatment at 500°C (Figure 3b) is similar, although the annealed sample should be free of organic residues according to the TGA measurement. Obviously, the removal of the organic components from between the nanowires leads to more compact structures, although without changing the macroscopic fibrous morphology. At temperatures of 700°C the nanowire bundles start to transform into pearl-necklace-like structures (Figure 3c) due to Rayleigh instability.[42] Whereas the crystal structure and the nanowire morphology remain unaltered in the sample annealed at 500°C, a calcination temperature of 700°C induces a change in the crystal structure to monoclinic WO_3 (see XRD and TEM data in the Supporting Information). Therefore, only the nanobundles after thermal treatment at 500°C were investigated with respect to their gas-sensing properties.

In general, CO and NO_2 are used as probe molecules to assess the gas-sensing properties of a new sensing material, mainly due to the simplicity of their detection mechanism, i.e., CO oxidation by adsorbed oxygen species to CO_2 and NO_2 ionosorption and formation of surface electron traps $NO^-_{2,ads}$, respectively. In our case, the tungsten oxide nanowires were nearly insensitive to CO in the concentration range between 1 and 10 ppm at all operating temperatures studied (the sensor signal R_{air}/R_{CO} was less than 2).

Figure 4a shows that the tungsten oxide nanowire sensors exhibit a high signal (≈ 9) at particularly low NO_2 concentrations of about 50 ppb (100 $\mu g\,m^{-3}$), which is a much better sensitivity than the recently reported SnO_2 and In_2O_3 nanowires.[37,39,40] This behavior can be explained by their high surface area and good crystallinity, combined with an

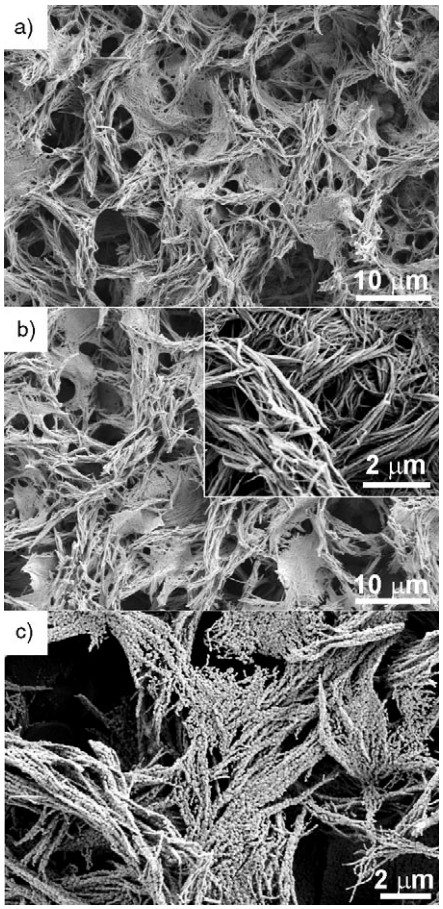

Figure 3. SEM images of the nanowire bundles deposited on the substrate at a) room temperature, b) after annealing at 500 °C (inset: higher magnification), and c) 700 °C.

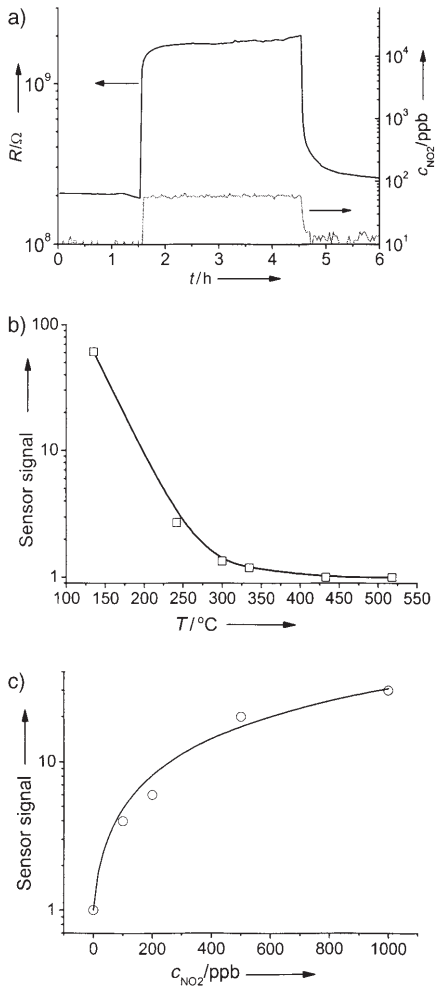

Figure 4. a) Black curve: change of the resistance R of the tungsten oxide nanowire bundles upon exposure to NO_2 ($\approx$50 ppb) at 150 °C in dry air; grey curve: NO_2 concentration measured simultaneously with an NO_x chemiluminescence analyzer. b) Dependence of the sensor signal ($S = R_{NO_2}/R_{air}$) to $\approx$100 ppb NO_2 on the operating temperature of the sensor in humid air (50% r.h. at 25 °C). c) Dependence of the sensor signal on NO_2 concentration in humid air (50% r.h. at 25 °C) (operating temperature of the sensors: 225 °C): experimental data points (○) and fitting curve based on the model from ref. [43]: $S = 1 + a\,C^b_{NO_2}$, fitting parameters: $a = (0.06 \pm 0.05)$ and $b = (0.89 \pm 0.13)$.

appropriate porosity of the deposited nanowire film, which provides good accessibility of the gases to the sensing layers. One should note, however, that at low operating temperatures of 150 °C the sensor is characterized by a relatively slow response and long recovery time. The sensor follows the profile of the NO_2 concentration as indicated by an on-line NO_x chemiluminescence analyzer (Figure 4a). Although the resistance of the layers (typically about 5 mm in diameter and several hundreds of nanometers thick) on conventional alumina substrates with low aspect ratio ($\approx$30) is very high ($\approx 10^8$ Ohm), this problem can be solved by using substrates with higher aspect ratios. The sensor signal of the tungsten oxide nanobundles is strongly dependent on the temperature (Figure 4b). Interestingly, the intensity of the signals decreases drastically with increasing operating temperature, leading to the observation that above 300 °C the nanobundles are nearly insensitive to NO_2. This behavior potentially enables the selective detection of reducing gases at higher temperatures. Generally, in the temperature range of 350–400 °C metal oxide sensors are sensitive to reducing gases such as hydrocarbons and volatile organic compounds. The calibration curves and the corresponding sensor signals and their dependence on NO_2 concentration can be approximated by power laws, as illustrated for an operating temperature of 200 °C in Figure 4c. The dependence of the sensor signal (S) on the NO_2 concentration (c_{NO_2}) can be described as $S = 1 + a\,c^b_{NO_2}$, where a and b are variables that can be fitted to $a = (0.06 \pm 0.05)$ and $b = (0.89 \pm 0.13)$. The experimental results correspond to the model developed by Gurlo et al.,[43] thus indicating the formation of surface-trapped states $NO_2^-{}_{,ads}$ (see also Figure 4c) with no evidence of dissociative NO_2 adsorption. The ionosorption of nitrogen dioxide at the surface of the tungsten oxide nanowires leads to the upward bending of the bands ($\approx$120 meV for 50 ppb NO_2 at 150 °C) and accordingly to an increase of the resistance, thus giving evidence for the n-type semiconducting properties of the tungsten oxide nanowires.

The controlled synthesis of one-dimensional tungsten oxide nanowires is particularly fascinating because bulk tungsten oxide exhibits manifold properties, including elec-

trochromism, semiconductivity, catalytic activity, and sensing properties. The present synthetic route can easily be performed in regular laboratory glassware and leads, at a low reaction temperature, directly to highly crystalline nanowires in good yields. This unique synthetic approach avoids any structure-directing agents as templates in the preparation of a high-purity nanomaterial. The nanobundles, which consist of self-assembled nanowires, can be separated into individual wires, thereby enabling dispersion as well as a rational interfacing of these nanobuilding blocks, either to other functional organic units or for chemical assembly into patterned arrays.

Their high surface-to-volume ratio combined with the high purity of the material makes these nanowire bundles ideal candidates for gas-sensing devices. This assumption is supported by initial results, which show an extraordinarily high sensitivity to low NO_2 concentrations. One major advantage of the good performance of the tungsten oxide sensor at low temperature is not only the possibility to fabricate low energy consuming devices, but also to tailor the gas-sensing properties of the nanobundles by in situ functionalization of the surface with specific organic and bioorganic receptors in order to provide high selectivity.

Received: August 9, 2005
Published online: November 28, 2005

Keywords: nanowires · organic–inorganic hybrid composites · oxides · sensors · tungsten

[1] X. F. Duan, Y. Huang, Y. Cui, J. F. Wang, C. M. Lieber, *Nature* **2001**, *409*, 66.
[2] C. N. R. Rao, F. L. Deepak, G. Gundiah, A. Govindaraj, *Prog. Solid State Chem.* **2003**, *31*, 5.
[3] Y. N. Xia, P. D. Yang, Y. G. Sun, Y. Y. Wu, B. Mayers, B. Gates, Y. D. Yin, F. Kim, Y. Q. Yan, *Adv. Mater.* **2003**, *15*, 353.
[4] C. N. R. Rao, B. Raveau, *Transition Metal Oxides*, VCH, New York, **1995**.
[5] Z. Y. Tang, N. A. Kotov, M. Giersig, *Science* **2002**, *297*, 237.
[6] J. Polleux, N. Pinna, M. Antonietti, M. Niederberger, *Adv. Mater.* **2004**, *16*, 436.
[7] J. Polleux, N. Pinna, M. Antonietti, C. Hess, U. Wild, R. Schlögl, M. Niederberger, *Chem. Eur. J.* **2005**, *11*, 3541.
[8] Z. Tang, N. A. Kotov, *Adv. Mater.* **2005**, *17*, 951.
[9] X. G. Peng, L. Manna, W. D. Yang, J. Wickham, E. Scher, A. Kadavanich, A. P. Alivisatos, *Nature* **2000**, *404*, 59.
[10] C. R. Martin, *Chem. Mater.* **1996**, *8*, 1739.
[11] M. Niederberger, M. H. Bartl, G. D. Stucky, *Chem. Mater.* **2002**, *14*, 4364.
[12] M. Niederberger, M. H. Bartl, G. D. Stucky, *J. Am. Chem. Soc.* **2002**, *124*, 13642.
[13] M. Niederberger, G. Garnweitner, F. Krumeich, R. Nesper, H. Cölfen, M. Antonietti, *Chem. Mater.* **2004**, *16*, 1202.
[14] M. Niederberger, N. Pinna, J. Polleux, M. Antonietti, *Angew. Chem.* **2004**, *116*, 2320; *Angew. Chem. Int. Ed.* **2004**, *43*, 2270.
[15] M. Niederberger, G. Garnweitner, N. Pinna, M. Antonietti, *J. Am. Chem. Soc.* **2004**, *126*, 9120.
[16] N. Pinna, G. Garnweitner, M. Antonietti, M. Niederberger, *Adv. Mater.* **2004**, *16*, 2196.
[17] N. Pinna, G. Neri, M. Antonietti, M. Niederberger, *Angew. Chem.* **2004**, *116*, 4445; *Angew. Chem. Int. Ed.* **2004**, *43*, 4345.
[18] N. Pinna, M. Antonietti, M. Niederberger, *Colloids Surf. A* **2004**, *250*, 211.
[19] N. Pinna, G. Garnweitner, P. Beato, M. Niederberger, M. Antonietti, *Small* **2005**, *1*, 113.
[20] N. Pinna, G. Garnweitner, M. Antonietti, M. Niederberger, *J. Am. Chem. Soc.* **2005**, *127*, 5608.
[21] J. Yang, C. Xue, S. H. Yu, J. H. Zeng, Y. T. Qian, *Angew. Chem.* **2002**, *114*, 4891; *Angew. Chem. Int. Ed.* **2002**, *41*, 4697.
[22] G. L. Frey, A. Rothschild, J. Sloan, R. Rosentsveig, R. Popovitz-Biro, R. Tenne, *J. Solid State Chem.* **2001**, *162*, 300.
[23] C. G. Granqvist, *Sol. Energy Mater. Sol. Cells* **2000**, *60*, 201.
[24] A. Tocchetto, A. Glisenti, *Langmuir* **2000**, *16*, 6173.
[25] W. Cheng, E. Baudrin, B. Dunn, J. I. Zink, *J. Mater. Chem.* **2001**, *11*, 92.
[26] G. Eranna, B. C. Joshi, D. P. Runthala, R. P. Gupta, *Crit. Rev. Solid State Mater. Sci.* **2004**, *29*, 111.
[27] O. Berger, T. Hoffmann, W.-J. Fischer, V. Melev, *J. Mater. Sci. Mater. Electron.* **2004**, *15*, 483.
[28] H. G. Choi, Y. H. Jung, D. K. Kim, *J. Am. Ceram. Soc.* **2005**, *88*, 1684.
[29] X. W. Lou, H. C. Zeng, *Inorg. Chem.* **2003**, *42*, 6169.
[30] K. Lee, W. S. Seo, J. T. Park, *J. Am. Chem. Soc.* **2003**, *125*, 3408.
[31] J.-W. Seo, Y.-W. Jun, S. J. Ko, J. Cheon, *J. Phys. Chem. B* **2005**, *109*, 5389.
[32] Z. Gu, Y. Ma, W. Yang, G. Zhang, J. Yao, *Chem. Commun.* **2005**, 3597
[33] J. Polleux, N. Pinna, M. Antonietti, M. Niederberger, *J. Am. Chem. Soc.* **2005**, *127*, 15595–15601.
[34] S. Iijima, T. Ichihashi, *Nature* **1993**, *363*, 603.
[35] M. Caravati, J.-D. Grunwaldt, A. Baiker, *Phys. Chem. Chem. Phys.* **2005**, *7*, 278.
[36] V. Augugliaro, S. Coluccia, V. Loddo, L. Marchese, G. Martra, L. Palmisano, M. Schiavello, *Appl. Catal. A* **1999**, *20*, 15.
[37] A. Kolmakov, M. Moskovits, *Annu. Rev. Mater. Res.* **2004**, *34*, 151.
[38] M. Law, H. Kind, B. Messer, F. Kim, P. D. Yang, *Angew. Chem.* **2002**, *114*, 2511; *Angew. Chem. Int. Ed.* **2002**, *41*, 2405.
[39] E. Comini, G. Faglia, G. Sberveglieri, Z. Pan, Z. L. Wang, *Appl. Phys. Lett.* **2002**, *81*, 1869.
[40] C. Li, D. Zhang, X. Liu, S. Han, T. Tang, J. Han, C. Zhou, *Appl. Phys. Lett.* **2003**, *82*, 1613.
[41] Y. L. Wang, X. C. Jiang, Y. N. Xia, *J. Am. Chem. Soc.* **2003**, *125*, 16176.
[42] M. E. T. Molares, A. G. Balogh, T. W. Cornelius, R. Neumann, C. Trautmann, *Appl. Phys. Lett.* **2004**, *85*, 5337.
[43] A. Gurlo, N. Bârsan, M. Ivanovskaya, U. Weimar, W. Göpel, *Sens. Actuators B* **1998**, *47*, 92.

